Vol. 2, No. 2, p. 190-209, 2018
www.astp-agr.com

Geo-Energy Research

Original article

Energy, exergy, and economic analysis of a geothermal power plant

Hamid Kazemi[1], M.A. Ehyaei[2]*

[1]*Department of Mechanical Engineering, South-Tehran Branch, Islamic Azad University, Tehran, Iran*

[2]*Department of Mechanical Engineering, Pardis Branch, Islamic Azad University, Pardis New City, Iran*

(Received January 1, 2018; revised April 3, 2018; accepted April 4, 2018; available online April 10, 2018)

Citation:
Kazemi, H., Ehyaei, M.A. Energy, exergy, and economic analysis of a geothermal power plant. *Advances in Geo-Energy Research*, 2018, 2(2): 190-209, doi: 10.26804/ager.2018.02.07.

Corresponding author:
*E-mail: aliehyaei@yahoo.com

Keywords:
Geothermal cycle
Organic Rankine Cycle
exergy

Abstract:
The current study aimed at designing a geothermal power plant in the Nonal area in Damavand district for simultaneous generation of thermal energy the electric power in the network of Damavand City and a part of Tehran province, the organic working fluid for the above cycle is R245fa which is a non-flammable fluid of dry type. The values of energy efficiency, exergy, the net rate of entropy change, and the specific output power were calculated as 18.2%, 21.3%, 172.97 kW/K, and 31.43 kJ/kg, respectively. The cost of drilling a well, as well as designing and construction of Damavand's geothermal power plant, were calculated to be 4.2 and 521.5 million (USD), respectively. Also, the cost per generation of each kW/h of power in Damavand power plant was 17 cents. The estimated payback time is calculated as 15 years. The analysis of the cycle in different months of the year showed that exergy efficiency has little change. The only significant effect of temperature changes was on the exergy efficiency as approximately a change of 2% can be seen during a year.

1. Introduction

Human has long sought to find a new opening to him by the use of the energies available in nature to besides facilitating its activities, carry out his tasks with the lowest costs and the highest speed, and take a step for more comfort and ease. The first energy used by the human is the sun's energy. Also, the people who had access to the free waters or lived in windy lands, used this kinetic energy and by transforming and controlling it, added to their ability for doing more difficult and bigger jobs. Another kind of energy which has been long known and used by the human is the geothermal energy. The people residing in the volcanic areas, either intentionally or unintentionally, somehow exploited this energy by the use of therapeutic characteristics of hot springs. With the increase in population and its expansion and dispersion, and also in line with the increasing need for new and more efficient energy with higher yields, the human gradually discovered fossil fuels and found it an inexhaustible source that promises a bright future (Ehyaei and Mozafari, 2010; Heberle and Brüggemann, 2010; Mozafari et al., 2010; Ehyaei et al., 2011, 2012; Ashari et al., 2012; Zarrouk and Moon, 2014). The human attachment to fossil fuels was ever increasing and in line with the improvements in the science and technology, and manufacturing several machines and tools, specifically the advent of industrial revolution, the use of this kind of fuel reached its highest level. Besides these improvements, the human gradually found out that in addition to limitations of fossil fuels, exploitation of this energy is not as cheap and soon, the consequences of burning fossil fuels became a new challenge for the communities. The rise in the need for energy and the limited resources of fossil fuels as well as their adverse environmental effects (including global warming) have led to increased efforts to use clean energy sources. The geothermal energy has a prominent place among the renewable energies due to vast resources on the ground (Lavizeh, 2002; Saidi et al., 2005b; Ehyaei and Bahadori, 2006, 2007; Ahmadi and Ehyaei, 2009; Ehyaei et al., 2010; Najafi and Ghobadian, 2011; Vélez et al., 2012; Ehyaei et al., 2013; Ghasemi et al., 2013; Astolfi et al., 2014; Ehyaei, 2014; Asgari and Ehyaei, 2015; Darvish et al., 2015; Saffari et al., 2016). So far, many studies have been conducted on the use of geothermal energy.

Kanoglu (2002) analyzed and investigated a double-stage double-surface geothermal power plant with a capacity of 12.4 MW, regarding exergy. The exergy loss in power plant includes the exergy lost by the working fluid in the condenser, the turbine-pump loss, and evaporator preheater. The exergy loss in these sites was 22.6%, 13.9%, and 13% of the total exergy

https://doi.org/10.26804/ager.2018.02.07.
2207-9963

input to the power plant, respectively. The exergy efficiency and thermal efficiency of the power plant based on the geothermal fluid exergy on the input of evaporator were calculated as 29.1% and 5.8%, respectively (e.g., the exergy input to the Rankine cycle). Drozdz in his study (2003), investigated the optimization method for transformation of geothermal energy. In this research, the optimization of the behavior of different types of geothermal energy source, which includes constant and dynamic parameters, is theoretically presented with a mathematical model based on the parameter of different qualities of well's water. The thermal energy production can be increased by the rise in the pumped water stream. The technical optimization method indicates that source the maximum net power which is the difference between the thermal source power and pumping power so that the maximum amount of thermal energy generated by the source minus the amount of electrical energy used for pumping. The results of the technical and economic optimization showed that the costs of the thermal energy unit are lower that electrical energy.

Ozgener et al. (2005) in their study analyzed and investigated a heating system with a geothermal source in Gonen district in Turkey (hydrothermal kind). The total energy and exergy efficiencies were evaluated by analysis and improvement of system performance, which were calculated as 45.9% and 64.1%, respectively.

Wei et al. (2007) in their study evaluated the improvement of the thermodynamic function of organic Rankine cycle. According to this study on optimization of the above cycle, five points are notable: the type of thermal source, selection of the working fluid, selection of the type of equipment to be used in the cycle, measures taken for controlling the cycle, and layout and size of its components. The thermal source can be geothermal energy, recycling of waste heat, solar energy or energy from combustion of biodiesel fuels. They considered the maximum use of heat from the geothermal source, which is one of the best ways to improve the performance of the organic alkaline cycle, important. In high air temperature, the produced power was reduced even up to 30%. Kanoglu et al. (2010) in their study dealt with analysis and investigation of thermodynamic models used for the production of hydrogen by geothermal energy. There are four methods developed for geothermal energy to be used for the production of hydrogen. These methods are: using the output heat from the geothermal fluid as the input power of an electrolysis process (Mode 1), use of geothermal heat to generate power for the electrolysis process and part of geothermal heat in an electrolysis process for preheated water (Mode 2), use of geothermal heat for preheated water in an electrolysis process with high temperature (Mode 3), and use of a part of geothermal power for electrolysis and the remainder to convert to fluid (Mode 4). The comparison between the amount of hydrogen produced in reversible and irreversible states indicates that exergy efficiency in the modes 1 to 4 is 28.5%, 29.9%, 37.2%, and 16.1%, respectively.

Arslan and Yetik (2011) in their study evaluated the optimization of a supercritical double-stage organic Rankine cycle with the geothermal source, using the Artificial Neural Network (ANN) algorithm, in Simaw district. In Simaw geothermal district, the highest profitability from the supercritical organic double-stage Rankine cycle with a capacity of 68.2 MW was obtained by the use of R744 organic working fluid and the values calculated for design parameters T_{1b}, T_{2a} and P_{2a} were 80 °C and 130 °C, and 12 MPa which was equal to 124.88 million USD. Jalilinasrabady et al. (2012) evaluated the optimization of Sabalan geothermal power plant's single-stage cycle by the use of the concept of exergy. The analyses of the proposed design indicated that if the separator and condenser pressures are 5.5 and 0.3 Bar respectively, the power plant's efficiency would be 31%. For obtaining the efficient optimal energy, a double-stage cycle was also evaluated for power generation. These conditions are given, if the pressure at the top of the cycle, bottom of the cycle, and the pressure on the condenser, are 7.5, 1.1 and 0.1 Bar respectively, the power plant's efficiency can reach to 49.7 MW. Enhua et al. (2012) examined the optimization and comparison of the efficiency of the organic Rankine cycle by recovering the waste heat from low-grade heat sources. The efficiency of five different types of organic Rankine cycles has been evaluated in this study. These configurations included the simple ORC, ORC with an internal heat exchanger, ORC with an open feed organic fluid heater, ORC with a closed feed organic fluid heater, and the ORC with a re-heater. Initially, they defined the functional area for the organic Rankine cycle and the internal combustion engine, and then they optimized the thermal efficiency of the organic Rankine cycle using a genetic algorithm. The combination of the first and second laws was used for evaluation and analysis of the specifications of each of the Rankine cycles. The analyses show that the ORC with an internal heat exchanger has the best thermodynamic efficiency. El-Emam and Dincer (2013) in a study dealt with thermodynamic and economic analysis and optimization of an ORC with geothermal source based on the energy and exergy concepts. Based on the analysis and investigation of the different temperatures of the geothermal water, the geothermal water's optimal function is at 165 °C. At this temperature, the energy and exergy efficiency is 16.4% and 48.8%, respectively. Bahrami et al. (2013) in a study dealt with the evaluation of the energy of the ORC for power generation by recovering heat wasted from low-grade heat sources with parabolic trough collectors taking into account the environmental considerations. They analyzed the cycle function and selected the suitable working fluid by the use of thermodynamic simulation. The effects of 12 different working fluids characteristics on the total efficiency of the cycle were evaluated and the results indicated that the normal decane fluid provides the highest efficiency in the mentioned cycle. Zhai et al. (2014) in their study elaborated on the selection of the suitable working fluid for ORC system. In this study, the effects of the characteristics of two working fluids from hydrocarbon and hydrofluorocarbon type on the system performance were evaluated. Also, a theoretical model was used for the cycle in order to optimize the evaporation temperature and maximize the produced power. The best working fluids for the source temperatures 383.15, 403.15 and 423.15 K were presented in the results of this study. Imran et al. (2015) in their study, investigated the multi-objective optimization of the heat exchanger of the ORC with

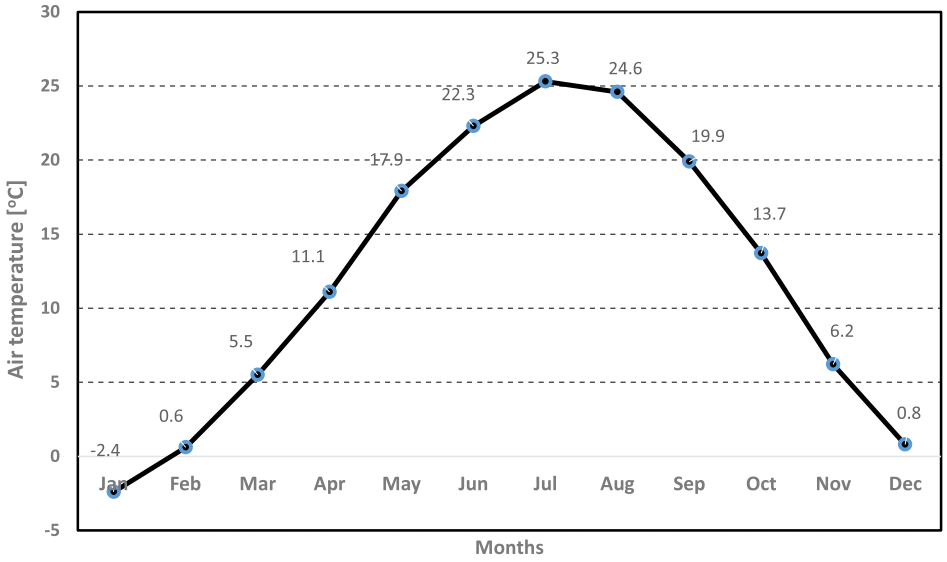

Fig. 1. Average monthly temperature for the Damavand area.

low temperature geothermal source. This study described a developed method of thermal and hydraulic design as well as optimization of geometric parameters and heat exchanger plate for an ORC with low temperature geothermal heat source. The minimum heat exchanger of 1570 USD is corresponding to a pressure drop of 125 kPa, while the maximum costs of 6988 USD is corresponding to a pressure drop of 5.2 kPa. Kazemi and Samadi (2016) in their study presented the economic, thermodynamic, and thermodynamic optimization of an ORC and provided a new design for ORC with geothermal source. They aimed at minimizing the investment costs for the cycle as well as maximizing the cycle's exergy efficiency. A new suggestion based on the three types of classic ORC, the regenerative ORC, and the steam double-stage ORC with geothermal source was introduced for increasing the power generation by the above cycle. By investigating the thermodynamic characteristics of different organic fluids, they chose isobutene an R123. Nami et al. (2017) in their study analyzed and interpreted the conventional and advanced exergy of double-stage ORC with geothermal source. The analysis of the normal exergy indicated that the low pressure heat exchanger, the high pressure heat exchanger, and the condenser are the most important components total exergy waste with 38.1%, 29.9% and 15.9% exergy waste, respectively.

Although many exergy and economic (2E) or exergy, economic and environmental (3E) analysis have been investigated about other kinds of power plants in the range of small to big sizes, no research has been done about the energy, exergy and economic analysis of geothermal power plant located in the special area of Iran. Also no detail energy, exergy, and economic analysis have been done on a combination systems of geothermal and ORC cycle in any place of Iran (Saidi et al., 2005a; Mozafari and Ehyaei, 2012; Yazdi et al., 2015a; Aliehyaei et al., 2015; Mohammadnezami et al., 2015; Yazdi et al., 2015b; Ehyaei and Farshin, 2017; Yousefi and Ehyaei, 2017; Ghasemian and Ehyaei, 2018).

The current study aimed at energy, exergy, and economic feasibility of an ORC with geothermal source, (hydrothermal type). Firstly, the costs of drilling a geothermal well as well as designing and erecting a geothermal power plant with a capacity of 100 MW in Nonal district of Damavand were evaluated, and then the single-stage evaporation ORC for the above power plant was selected. After designing the above cycle, all key parameters of the power plant were calculated. The innovations of this research are:

- The precise and comprehensive study on energy, exergy, and economic feasibility of geothermal power plant (hydrothermal kind) in Nonal district of Damavand.
- Evaluation of the first and second law efficiencies of the above power plant in different seasons.

2. Selection of thermodynamic cycle suitable for geothermal reservoir

The geothermal reservoir is located on the outskirt of Mount Damavand, north of Iran. Type of geothermal reservoir is hydrothermal. Mount Damavand is known as the highest mountain in Iran and the highest volcano in the Middle East. This mountain is located in the central part of the Alborz mountain range in the south of the Caspian Sea and the Larijan section of Amol city in Mazandaran province with a 66 km distance to Tehran. This mountain is located 69 km off the north-east of Tehran, 62 km off the southwest of Amol, and 26 km off the northwest of Damavand city. Fig. 1 shows the average monthly temperature for the Damavand area (Dabirsiaghi, 2013).

Damavand is a volcanic mountain formed mainly during the fourth geological period, called the Holocene, and is of stratified volcano type (silent volcanic) which is relatively young. The volcanic activity of this mountain is currently

Table 1. Number and the average depth of the wells in Damavand Geothermal Power Plant.

Number of the Damavand Power Plant Wells	14	-	-
Number of productive wells	8	(m)	2000-3000
Number of the used productive wells	6	(m)	2000-3000
Number of the reserved productive wells	2	(m)	2000-3000
Number of injection wells	2	(m)	1000
Number of cold water supply wells	4	(m)	100-130

limited to the sublimation of sulfur gases. The last volcanic activity of this mountain was 38,500 years ago. Now the mountain is a dormant volcano that can be re-activated. According to the website of the National Iranian Statistics, the peak's height is 5610 m. The diameter of the crater of the volcano is about 400 m. The central part of the crater is covered by a lake of ice, and on the sidelines there are chimneys that make the surrounding land yellow. Apart from the current crater, there is the evidence of the old crater, one of which is located at the southern side and at an altitude of 100 m, which is now the location of gases and smoke exits. The average rainfall in the Damavand heights is 1400 mm per year and it is mainly snow in the highlands. Thus, the volcanic rocks in the area are the Damavand geothermal reservoir's heat source. One of the most important components of a geothermal reservoir is the fluid (hot water or steam) which must be penetrated by special passages. The average rainfall in Damavand area is more than 1400 mm per year which is a significant amount. An abundant number of faults, seams, and gaps in the area have also provided suitable channels for atmospheric precipitation penetration into the reservoir (Dabirsiaghi, 2013). Geothermal sources of Iran are of water-lifting and hydrothermal systems type. Based on the above explanations, it is shown that the conditions of a high-temperature geothermal reservoir in the Damavand region are well prepared. The proximity to Damavand city and the province of Tehran, the most populous province and capital of the country, has greatly increased the importance of this geothermal reservoir. Thermal capacity of Damavand reservoir is predicted to be around 180 MWT. However, the updated model of the reservoir indicates that its thermal capacity 30% more than the predictions. Based on the geochemical studies, the hot water springs and the use of Chemical geothermometers, the reservoir's temperature is around 150 to 210 ^{o}C. The reservoir's pressure is predicted to be 15 to 80 Bar for which the 45 Bar is considered as the average pressure. The geothermal power plant's efficiency is generally very low and ranges from 10 to 20%, which is about a third of the efficiency of the fossil and nuclear power plants (Dabirsiaghi, 2013). The reasons behind this lowness are the lower temperatures, lower steam pressure, and the chemical combinations of geothermal steam, which is different with the pure water steam and includes variable quantities of non-condensing gases, such as (N_2, H_2, CH_4, NH_3, H_2S, CO_2), that lead to a discrepancy in the process of power generation and thus reducing the efficiency. When the geothermal steam includes more than 10 non-condensing gases, the use of condenser is not economic anymore. In this case, a direct system with no condenser will be used. In this cycle, the geothermal steam is directly input to the turbine and its output is entered into the atmosphere. The presence of condenser plays a significant role in the amount of steam needed for turbine capacity. However, in the power plant with direct cycle and without condenser, 15 to 20 kg of steam is consumed per generation of 1 kWh of power, while for the power plant with condenser and cooling tower, it is 6 to 10 kg. The amount of consumed steam is directly related to the number of wells and as a result, plays a significant role in drilling costs. The geothermal plant has a capacity coefficient of about 80% (Dabirsiaghi, 2013). Regarding these initial data, the single-stage steam ORC for the Damavand Power Plant can be considered. The constant single-stage evaporation system with condenser is simpler than the double-stage system since it does not require a secondary fluid and a secondary fluid pump. In addition, the costs of the plant equipment in constant evaporation system is significantly lower than those of double-stage system. The double-stage system has a more sophisticated technology, since the secondary fluid, like Freon and Isobutene, etc., is volatile and is often toxic and flammable and therefore should be prevented from entering the atmosphere. The biggest advantage of power plants with double-stage system, as compared to the system with immediate evaporation, is its operational scope in terms of the geothermal fluid's temperature which can generate power from the hot water sources with low temperatures to temperatures up to 85^{o}C, while the operational scope of the systems with immediate evaporation is about 140^{o}C and above, and even in this scope, the immediate evaporation system is economic (Dabirsiaghi, 2013).

3. Main components of geothermal reservoir

In order to construct this plant, at least 14 wells should be drilled in the Nonal Region in Damavand, which include eight production wells with a depth of between 2000 and 3000 m, two injection wells with a depth of between 2000 and 3000 m, and four wells for provision of cold water to the power plant, with a depth of 100 to 130 m. The area of the well's drilling field is about 104 km^2. According to the information from the related resources, the reservoir temperature is predicted to be 150 to 210 ^{o}C. The reservoir's pressure is also measured as 15 to 80 Bar, for which 45 Bar is considered as an average. The Table 1 and Table 2 show the number and the average depth of the plant's wells, and the thermodynamic specifications of

Table 2. Thermodynamic specifications of the Damavand's geothermal reservoir.

Geothermal reservoir temperature	$T_{Reservoir}$	(^{o}C)	150-210
Damavand's geothermal reservoir pressure	$P_{Reservoir}$	(Bar)	15-80
Geothermal reservoir's average pressure	$P_{av.Reservoir}$	(Bar)	45

Table 3. Specifications of Damavand Geothermal Power Plant's cold water reservoirs.

Cold water reservoir of Damavand Power Plant	$Reservoir_{cw}$	-	2
The capacity of the cold water reservoirs	-	(m^3)	100
The flow discharge of cold water output from the well	$\dot{m}_{cw}$	(lit/s)	220

the geothermal reservoir, respectively.

The underground cold water pumping station is located 2.6 km from the power plant and near it. The cold water is supplied by four wells. The approximate depth of the wells is between 100 and 130 m, each having a discharge of more than 220 Lit/S. The cold water is transferred from the wells to two reservoirs with each having a capacity of 50 m^3, through the pipes, and then it is sent from the reservoirs to the condensers, heat exchangers, and aerosol generators, by a pump. Table 3 shows the specifications of Damavand Geothermal Power Plant's cold water reservoirs.

4. Energy and exergy model of geothermal power plant

The thermodynamic analysis of the Damavand Geothermal Power Plant is as follows. The assumptions are as below:

1) The location of the study is chosen in Tehran and near Nonal district of Damavand City regarding the geothermal potentials of Iran.

2) The average temperature of Damavand City has been considered 12.1 ^{o}C according to information provided by the Meteorology Center.

3) The process is steady state.

4) The heat wasted is about 5%, and pressure drop is 3%.

5) The process in turbine and pump is of polytropic type.

6) The condenser and evaporator's efficiency is taken as 80%.

7) The isentropic efficiency of the turbine and the pump are considered 85%.

8) The heat exchange with low-temperature source is done at the constant temperature of 30 ^{o}C.

9) The geothermal fluid temperature is always constant and equal to 150 ^{o}C and 4 Bar.

10) Type of geothermal system is hydrothermal.

The Fig. 2 shows a schematic design of Damavand geothermal power plant single-stage steam ORC. A certain amount of geothermal fluid is initially converted into a two-phase fluid during its mast process (after passing through the geothermal tubes and the heat absorption from the ground) in which the pressure drop in the enthalpy is constant. A certain amount of geothermal fluid is initially converted into a two-phase fluid during the choking process (after passing through the geothermal tubes and the heat absorption from the ground) in which we have an immediate pressure drop in the enthalpy. The two-phase fluid is entered into the separator, and the fluid saturation steam is input to the turbine 1 from the path number 7. In a constant temperature and pressure process, the saturated steam expands and rotates the turbine 1's blades which leads to the generation of power by the generator. It leads to the pressure drop and reduction in the saturated steam temperature, which may also cause a slight condensation. The wet steam output from the turbine 1 loses its heat and pressure, and enters the condenser 1, converting into the saturated fluid by the cold water provided by the cooling tower, after transferring into the condenser 1, and then the distillation is done. Through the distillation of the wet steam in condenser 1, a vacuum between the turbine and the condenser is created and the pressure after the turbine is reduced, while the turbine rotation ability is increased, to beside rising the plant's efficiency, increase the power generation amount. The saturated fluid output from the condenser 1 returns to the earth's layers at a low pressure. On the path number 8, the saturated fluid separated by the separator, before mixing with the saturated fluid output from the condenser 1 and returning to earth's layers, gives its thermal energy to an ORC with R245fa organic working fluid. The saturated fluid input to the heat exchanger converts to the dry saturated steam through a constant pressure process, by a geothermal heat source. The dry saturated fluid output from the heat exchanger is guided towards the turbine 2, and in a constant temperature and pressure process, the turbine's blades are rotated by the expanded dry saturated steam, which leads to power generation by the generator. This operation reduces the pressure and temperature of the saturated steam, which may also cause a slight condensation. The wet steam output from the turbine number 2 loses its temperature and pressure and enters the condenser number 2 where it converts to the saturated fluid by the cold water from the cooling tower which is pumped into this condenser and then the distillation is done. By distillation of the saturated steam in condenser number 2, a vacuum is created between the turbine and condenser, and the pressure after turbine is reduced while the turbine rotation power is increased to, besides rising the power plant's efficiency, increase the power generation level. The saturated fluid output from the condenser in low pressure is pumped to a higher pressure, and it enters the heat exchanger with

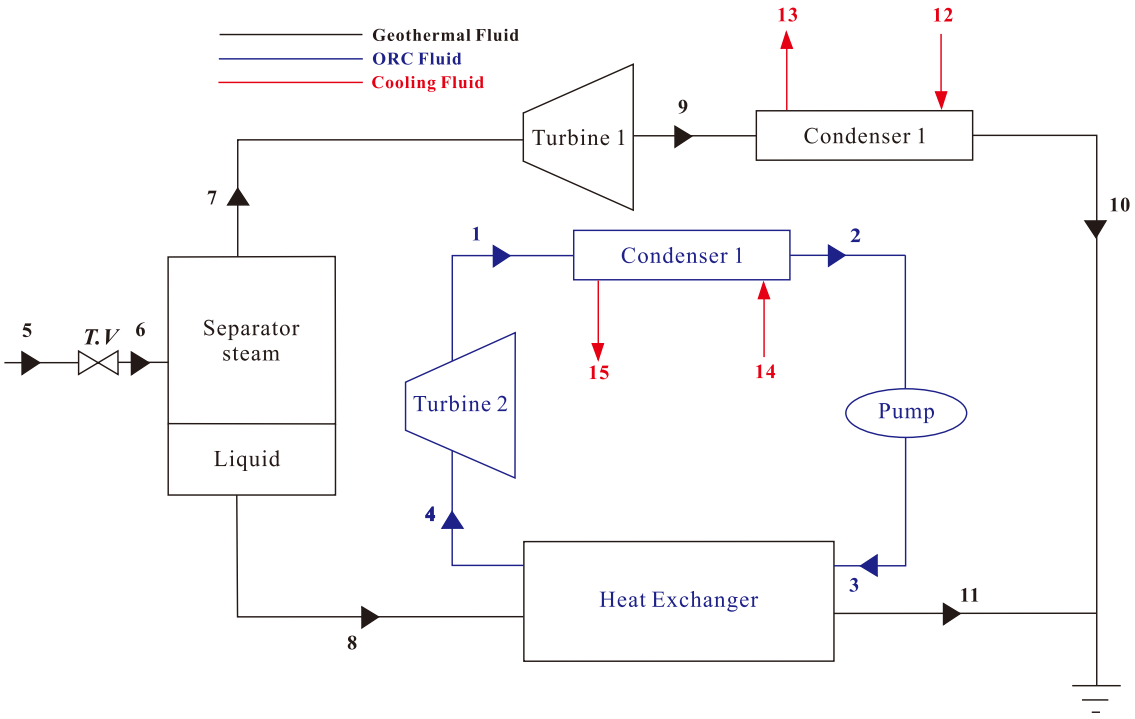

Fig. 2. Single-stage steam ORC of Damavand Geothermal Power Plant.

high pressure and heat, and the ORC power generation cycle with the geothermal heat source is run again (Golroodbari and Kalte, 2013).

The mass and energy equations of the pump are as follows (Bejan et al., 2006):

$$\dot{m}_2 = \dot{m}_3 \tag{1}$$

$$\dot{W}_{Pump} = \left[\frac{\dot{m}_2}{\eta_{Pump}}\left(h_3 - h_2\right)\right] \tag{2}$$

$$\eta_{Pump} = \left(\frac{h_{3.is} - h_2}{h_3 - h_2}\right) \tag{3}$$

where $\dot{W}_{Pump}$ and η_{Pump} are pump power value per kW and the pump first law efficiency per percent, respectively; $\dot{m}_2$ and $\dot{m}_3$ are the mass flow rate of pump inlet and outlet , kg/s; h_2 and h_3 are the pump inlet and outlet enthalpy, kJ/kg; and the is subscript also means isentropic.

The conservation of mass and energy equations of turbine 1 are as follows:

$$\dot{m}_7 = \dot{m}_9 \tag{4}$$

$$\dot{W}_{Turbine.1} = \dot{m}_7 \times \eta_{Turbine.1}\left(h_7 - h_9\right) \tag{5}$$

$$\eta_{Turbine.1} = \left(\frac{h_7 - h_9}{h_7 - h_{9.is}}\right) \tag{6}$$

where $\dot{W}_{Turbine.1}$ and $\eta_{Turbine.1}$ are turbine 1 power amount and efficiency per kW, respectively; $\dot{m}_7$ and $\dot{m}_9$ are the turbine 1's inlet and outlet mass discharge, kg/s; h_7 and h_9 are the turbine 1's inlet and outlet enthalpy, kJ/kg; and the is subscript also means isentropic.

The conservation of mass and energy equations of turbine 2 are as follows (Bejan et al., 2006):

$$\dot{m}_4 = \dot{m}_1 \tag{7}$$

$$\dot{W}_{Turbine.2} = \dot{m}_4 \times \eta_{Turbine.2}\left(h_4 - h_1\right) \tag{8}$$

$$\eta_{Turbine.2} = \left(\frac{h_4 - h_1}{h_4 - h_{1.is}}\right) \tag{9}$$

where $\dot{W}_{Turbine.2}$ and $\eta_{Turbine.2}$ are turbine 2 power amount and efficiency per kW, respectively; $\dot{m}_4$ and $\dot{m}_1$ are the turbine 2's inlet and outlet mass discharge, kg/s; h_4 and h_1 are the turbine 2's inlet and outlet enthalpy, kJ/kg; and the is subscript also means isentropic.

The conservation of mass and energy equations of heat exchanger are as follows (Bejan et al., 2006):

$$\dot{m}_8 + \dot{m}_3 = \dot{m}_{11} + \dot{m}_4 \tag{10}$$

$$\dot{Q}_{Evaporator} = \dot{m}_3\left(h_4 - h_3\right) \tag{11}$$

$$\dot{Q}_{Geothermal.in} = \dot{m}_8\left(h_8 - h_{11}\right) \tag{12}$$

where $\dot{Q}_{Geothermal.in}$ is the geothermal fluid temperature, kW; $\dot{Q}_{Evaporator}$ is the heat exchanger temperature, kW; $\dot{m}_3$ and $\dot{m}_8$ are the heat exchanger inlet mass discharge, kg/s; $\dot{m}_4$ and $\dot{m}_{11}$ are the heat exchanger outlet mass discharge, kg/s; h_3 and h_8 are the heat exchanger inlet enthalpy, kJ/kg; h_4 and h_{11} are the heat exchanger outlet enthalpy, kJ/kg.

The conservation of mass and energy equations of condenser 1 are as follows (Bejan et al., 2006):

$$\dot{m}_9 = \dot{m}_{10}, \dot{m}_{12} = \dot{m}_{13} \tag{13}$$

$$\dot{Q}_{condenser.1} = \dot{m}_9 \left(h_9 - h_{10}\right) \tag{14}$$

$$\dot{Q}_{condenser.1} = \dot{m}_{12} \left(h_{13} - h_{12}\right) \tag{15}$$

where $\dot{Q}_{condenser.1}$ is the condenser 1's temperature, kW; $\dot{m}_9$ and $\dot{m}_{12}$ are the condenser 1's inlet mass discharge, kg/s; $\dot{m}_{10}$ and $\dot{m}_{13}$ are the condenser 1's outlet mass discharge, kg/s; h_9 and h_{12} are the condenser 1's inlet enthalpy, kJ/kg; h_{10} and h_{13} are the condenser 1's outlet enthalpy, kJ/kg.

The conservation of mass and energy equations of condenser 2 are as follows (Bejan et al., 2006):

$$\dot{m}_1 + \dot{m}_{14} = \dot{m}_2 + \dot{m}_{15} \tag{16}$$

$$\dot{Q}_{condenser.2} = \dot{m}_1 \left(h_1 - h_2\right) \tag{17}$$

$$\dot{Q}_{condenser.2} = \dot{m}_{14} \left(h_{15} - h_{14}\right) \tag{18}$$

where $\dot{Q}_{condenser.2}$ is the condenser 2's temperature, kW; $\dot{m}_1$ and $\dot{m}_{14}$ are the condenser 2's inlet mass discharge, kg/s; $\dot{m}_2$ and $\dot{m}_{15}$ are the condenser 2's outlet mass discharge, kg/s; h_1 and h_{14} are the condenser 2's inlet enthalpy, kJ/kg; h_2 and h_{15} are the condenser 2's outlet enthalpy, kJ/kg.

The conservation of mass and energy equations of the separator are as follows (Bejan et al., 2006):

$$\dot{m}_6 = \dot{m}_7 + \dot{m}_8 \tag{19}$$

$$\dot{Q}_{Separator} = \dot{m}_6 \left(h_7 - h_6\right) = \dot{m}_6 \left(h_8 - h_6\right) \tag{20}$$

where $\dot{Q}_{Separator}$ is the separator's temperature, kW; $\dot{m}_6$ is the separator's inlet mass discharge, kg/s; $\dot{m}_7$ and $\dot{m}_8$ are the separator's outlet mass discharge, kg/s; h_6 is the separator's inlet enthalpy, kJ/kg; h_7 and h_8 are the separator's outlet enthalpy, kJ/kg.

The conservation of mass and energy equations of the tap valve are as follows (Bejan et al., 2006):

$$\dot{m}_5 = \dot{m}_6 \tag{21}$$

$$\dot{Q}_{T.V} = \dot{m}_5 \left(h_6 - h_5\right) \tag{22}$$

$$\dot{Q}_{T.V} = 0 \tag{23}$$

where $\dot{Q}_{T.V}$ is the tap valve temperature, kW; $\dot{m}_5$ and $\dot{m}_6$ are the tap valve inlet and outlet mass discharge, kg/s; h_5 and h_6 are the tap valve inlet and outlet enthalpy, kJ/kg. Since the tap valve is considered to be adiabatic, therefore $\dot{Q}_{T.V} = 0$.

The thermal efficiency equations for the first law and the specific output power are as follows (Bejan et al., 2006):

$$\eta_{th} = \left[\frac{\dot{W}_{net}}{\dot{Q}_{Geothermal.in}}\right] \tag{24}$$

$$\eta_{th} = \left[\frac{\left[\left(\dot{W}_{Turb.1} + \dot{W}_{Turb.2}\right) - \dot{W}_{Pump}\right]}{\dot{Q}_{Geothermal.in}}\right] \tag{25}$$

$$w = \left[\frac{\left[\left(\dot{W}_{Turb.1} + \dot{W}_{Turb.2}\right) - \dot{W}_{Pump}\right]}{\dot{m}}\right] \tag{26}$$

where η_{th} is the first law thermal efficiency, %; $\dot{Q}_{Geothermal.in}$ is the geothermal fluid temperature, kW; $\dot{W}_{Turb.1}$, $\dot{W}_{Turb.2}$, $\dot{W}_{Pump}$ and $\dot{W}_{net}$ are turbine 1, turbine 2, pump and net power, respectively, kW; w is the specific output power, kJ/kg; and $\dot{m}$ is the mass discharge, kg/s.

The equations of pump exergy are as follows (Jafari et al., 2012):

$$\dot{E}_{S.Pump} = \dot{m}_2 \left(e_3 - e_2\right) - \dot{W}_{Pump} \tag{27}$$

$$\dot{S}_{gen.Pump} = \dot{m}_2 \left(s_3 - s_2\right) \tag{28}$$

$$\dot{I} = T_0 \times \dot{S}_{gen.Pump} = \dot{m}_2 \times T_0 \left(s_3 - s_2\right) \tag{29}$$

where $\dot{E}_{S.Pump}$ is the pump exergy flow, kW; $\dot{W}_{Pump}$ is the pump power, kW; $\dot{S}_{gen.Pump}$ is the pump net rate of entropy change, kW/K; e_2 and e_3 are the pump inlet and outlet exergy, kJ/kg; $\dot{m}_2$ is the pump inlet mass discharge, kg/s; s_2 and s_3 are the pump inlet and outlet entropy, kJ/(kg·K); T_0 is the ambient temperature; and $\dot{I}$ is the pump exergy waste, kW.

The equations of turbine 1's exergy are as follows (Jafari et al., 2012):

$$\dot{E}_{S.Turbine.1} = \dot{m}_7 \left(e_9 - e_7\right) - \dot{W}_{Turbine.1} \tag{30}$$

$$\dot{S}_{gen.Turbine.1} = \dot{m}_7 \left(s_9 - s_7\right) \tag{31}$$

$$\dot{I} = T_0 \times \dot{S}_{gen.Turbine.1} = \dot{m}_7 \times T_0 \left(s_9 - s_7\right) \tag{32}$$

where $\dot{E}_{S.Turbine.1}$ is the turbine 1's exergy flow, kW; $\dot{W}_{Turbine.1}$ is the turbine 1's power, kW; $\dot{S}_{gen.Turbine.1}$ is the turbine 1's net rate of entropy change, kW/K; e_7 and e_9 are the turbine 1's inlet and outlet exergy, kJ/kg; $\dot{m}_7$ is the turbine 1's inlet mass discharge, kg/s; s_7 and s_9 are the turbine 1's inlet and outlet entropy, kJ/(kg·K); T_0 is the ambient temperature; and $\dot{I}$ is the turbine 1's exergy waste, kW.

The equations of turbine 2's exergy are as follows (Jafari et al., 2012):

$$\dot{E}_{S.Turbine.2} = \dot{m}_4 (e_1 - e_4) - \dot{W}_{Turbine.2} \tag{33}$$

$$\dot{S}_{gen.Turbine.2} = \dot{m}_4 (s_1 - s_4) \tag{34}$$

$$\dot{I} = T_0 \times \dot{S}_{gen.Turbine.2} = \dot{m}_4 \times T_0 (s_1 - s_4) \tag{35}$$

where $\dot{E}_{S.Turbine.2}$ is the turbine 2's exergy flow, kW; $\dot{W}_{Turbine.2}$ is the turbine 2's power, kW; $\dot{S}_{gen.Turbine.2}$ is the turbine 2's net rate of entropy change, kW/K; e_4 and e_1 are the turbine 2's inlet and outlet exergy, kJ/kg; $\dot{m}_4$ is the turbine 2's inlet mass discharge, kg/s; s_4 and s_1 are the turbine 2's inlet and outlet entropy, kJ/(kg·K); T_0 is the ambient temperature; and $\dot{I}$ is the turbine 2's exergy waste, kW.

The equations of evaporator exergy are as follows (Jafari et al., 2012):

$$\dot{E}_{S.Evaporator} = \dot{m}_3 (e_4 - e_3) + \left[\left(1 - \frac{T_0}{T_{Eva}} \right) \dot{Q}_{Evaporator} \right] \tag{36}$$

$$\begin{aligned} \dot{S}_{gen.Evaporator} &= \dot{m}_3 (s_4 - s_3) - \left(\frac{\dot{Q}_{Eva}}{T_0} \right) \\ &= \dot{m}_3 \left[s_4 - s_3 - \left(\frac{\dot{Q}_{Evaporator}}{T_{Source}} \right) \right] \end{aligned} \tag{37}$$

$$\dot{S}_{gen.Evaporator} = \dot{m}_3 \left[s_4 - s_3 - \left(\frac{h_4 - h_3}{T_{Source}} \right) \right] \tag{38}$$

$$\begin{aligned} \dot{I} &= T_0 \times \dot{S}_{gen.Evaporator} \\ &= \dot{m}_3 \times T_0 \left[s_4 - s_3 \left(\frac{h_4 - h_3}{T_{Source}} \right) \right] \end{aligned} \tag{39}$$

where $\dot{E}_{S.Evaporator}$ is the evaporator exergy flow, kW; T_0 and $T_{Evaporator}$ are ambient temperature and evaporator temperature, respectively, K; $\dot{Q}_{Evaporator}$ is the evaporator heat level, kW; $\dot{S}_{gen}$ is the evaporator net rate of entropy change, kW/K; e_3 and e_4 are the evaporator inlet and outlet exergy, kJ/kg; $\dot{m}_3$ is the evaporator inlet mass discharge, kg/s; s_3 and s_4 are the evaporator inlet and outlet entropy, kJ/(kg·K); h_3 and h_4 are the evaporator inlet and outlet enthalpy, kJ/kg; $\left(\frac{\dot{Q}_{Eva}}{T_0} \right)$ is the heat exchanged between the evaporator and environment, kW; and $\dot{I}$ is the evaporator exergy waste, kW.

The equations of condenser 1's exergy are as follows (Jafari et al., 2012):

$$\begin{aligned} \dot{E}_{S.Condenser.1} &= \dot{m}_9 (e_{10} - e_9) \\ &+ \left[\left(1 - \frac{T_0}{T_{Cond.1}} \right) \dot{Q}_{Condenser.1} \right] \end{aligned} \tag{40}$$

$$\begin{aligned} \dot{S}_{gen.Condenser.1} &= \dot{m}_9 (s_{10} - s_9) - \left(\frac{\dot{Q}_{Cond.1}}{T_0} \right) \\ &= \dot{m}_9 \left[s_{10} - s_9 - \left(\frac{\dot{Q}_{Condenser.1}}{T_{Sink}} \right) \right] \end{aligned} \tag{41}$$

$$\dot{S}_{gen.Condenser.1} = \dot{m}_9 \left[s_{10} - s_9 - \left(\frac{h_9 - h_{10}}{T_{Sink}} \right) \right] \tag{42}$$

$$\begin{aligned} \dot{I} &= T_0 \times \dot{S}_{gen.Condenser.1} \\ &= \dot{m}_9 \times T_0 \left[s_{10} - s_9 \left(\frac{h_9 - h_{10}}{T_{Sink}} \right) \right] \end{aligned} \tag{43}$$

where $\dot{E}_{S.Condenser.1}$ is the condenser 1's exergy flow, kW; T_0 and $T_{Condenser.1}$ are ambient temperature and condenser 1's temperature, respectively, K; $\dot{Q}_{Condenser.1}$ is the condenser 1's heat level, kW; $\dot{S}_{gen.Condenser.1}$ is the condenser 1's net rate of entropy change, kW/K; e_9 and e_{10} are the condenser 1's inlet and outlet exergy, kJ/kg; $\dot{m}_9$ is the condenser 1's inlet mass discharge, kg/s; s_9 and s_{10} are the condenser 1's inlet and outlet entropy, kJ/(kg·K); h_9 and h_{10} are the condenser 1's inlet and outlet enthalpy, kJ/kg; $\left(\frac{\dot{Q}_{Cond.1}}{T_0} \right)$ is the heat exchanged between the condenser 1 and environment, kW; and $\dot{I}$ is the condenser 1's exergy waste, kW.

The equations of condenser 2's exergy are as follows (Jafari et al., 2012):

$$\begin{aligned} \dot{E}_{S.Condenser.2} &= \dot{m}_1 (e_2 - e_1) \\ &+ \left[\left(1 - \frac{T_0}{T_{Cond.2}} \right) \dot{Q}_{Condenser.2} \right] \end{aligned} \tag{44}$$

$$\begin{aligned} \dot{S}_{gen.Condenser.2} &= \dot{m}_1 (s_2 - s_1) - \left(\frac{\dot{Q}_{Cond.2}}{T_0} \right) \\ &= \dot{m}_1 \left[s_2 - s_1 - \left(\frac{\dot{Q}_{Condenser.2}}{T_{Sink}} \right) \right] \end{aligned} \tag{45}$$

$$\dot{S}_{gen.Condenser.2} = \dot{m}_1 \left[s_2 - s_1 - \left(\frac{h_1 - h_2}{T_{Sink}} \right) \right] \tag{46}$$

$$\begin{aligned} \dot{I} &= T_0 \times \dot{S}_{gen.Condenser.2} \\ &= \dot{m}_1 \times T_0 \left[s_2 - s_1 \left(\frac{h_1 - h_2}{T_{Sink}} \right) \right] \end{aligned} \tag{47}$$

where $\dot{E}_{S.Condenser.2}$ is the condenser 2's exergy flow, kW; T_0 and $T_{Condenser.2}$ are ambient temperature and condenser 2's temperature, respectively, K; $\dot{Q}_{Condenser.2}$ is the condenser 2's heat level, kW; $\dot{S}_{gen.Condenser.2}$ is the condenser 2's net rate of entropy change, kW/K; e_1 and e_2 are the condenser 2's inlet and outlet exergy, kJ/kg; $\dot{m}_1$ is the condenser 2's inlet mass discharge, kg/s; s_1 and s_2 are the condenser 2's inlet and

outlet entropy, kJ/(kg·K); h_1 and h_2 are the condenser 2's inlet and outlet enthalpy, kJ/kg; $\left(\frac{\dot{Q}_{Cond.2}}{T_0}\right)$ is the heat exchanged between the condenser 2 and environment, kW; and $\dot{I}$ is the condenser 2's exergy waste, kW.

The equations of separator exergy are as follows (Jafari et al., 2012):

$$\dot{E}_{S.Separator} = \dot{m}_6 (e_7 - e_6) + \left[\left(1 - \frac{T_0}{T_{Separator}}\right)\dot{Q}_{Separator}\right] \quad (48)$$

$$\dot{S}_{gen.Separator} = \dot{m}_6 (s_7 - s_6) - \left(\frac{\dot{Q}_{Separator}}{T_0}\right) = \dot{m}_6 \left[s_7 - s_6 - \left(\frac{\dot{Q}_{Separator}}{T_{Source}}\right)\right] \quad (49)$$

$$\dot{S}_{gen.Separator} = \dot{m}_6 \left[s_7 - s_6 - \left(\frac{h_7 - h_6}{T_{Source}}\right)\right] \quad (50)$$

$$\dot{I} = T_0 \times \dot{S}_{gen.Separator} = \dot{m}_6 \times T_0 \left[s_7 - s_6 \left(\frac{h_7 - h_6}{T_{Source}}\right)\right] \quad (51)$$

where $\dot{E}_{S.Separator}$ is the separator exergy flow, kW; T_0 and $T_{Separator}$ are ambient temperature and separator temperature, respectively, K; $\dot{Q}_{Separator}$ is the separator heat level, kW; $\dot{S}_{gen.Separator}$ is the separator net rate of entropy change, kW/K; e_6 and e_7 are the separator inlet and outlet exergy, kJ/kg; $\dot{m}_6$ is the separator inlet mass discharge, kg/s; s_6 and s_7 are the separator inlet and outlet entropy, kJ/(kg·K); h_6 and h_7 are the separator inlet and outlet enthalpy, kJ/kg; $\left(\frac{\dot{Q}_{Separator}}{T_0}\right)$ is the heat exchanged between the separator and environment, kW; and $\dot{I}$ is the separator exergy waste, kW.

Equation for liquid seperation is as follows:

$$\dot{E}_{S.Separator} = \dot{m}_6 (e_8 - e_6) + \left[\left(1 - \frac{T_0}{T_{Separator}}\right)\dot{Q}_{Separator}\right] \quad (52)$$

$$\dot{S}_{gen.Separator} = \dot{m}_6 (s_8 - s_6) - \left(\frac{\dot{Q}_{Separator}}{T_0}\right) = \dot{m}_6 \left[s_8 - s_6 - \left(\frac{\dot{Q}_{Separator}}{T_{Source}}\right)\right] \quad (53)$$

$$\dot{S}_{gen.Separator} = \dot{m}_6 \left[s_8 - s_6 - \left(\frac{h_8 - h_6}{T_{Source}}\right)\right] \quad (54)$$

$$\dot{I} = T_0 \times \dot{S}_{gen.Separator} = \dot{m}_6 \times T_0 \left[s_8 - s_6 \left(\frac{h_8 - h_6}{T_{Source}}\right)\right] \quad (55)$$

where $\dot{E}_{S.Separator}$ is the separator exergy flow, kW; T_0 and $T_{Separator}$ are ambient temperature and separator temperature, respectively, K; $\dot{Q}_{Separator}$ is the separator heat level, kW; $\dot{S}_{gen.Separator}$ is the separator net rate of entropy change, kW/K; e_6 and e_8 are the separator inlet and outlet exergy, kJ/kg; $\dot{m}_6$ is the separator inlet mass discharge, kg/s; s_6 and s_8 are the separator inlet and outlet entropy, kJ/(kg·K); h_6 and h_8 are the separator inlet and outlet enthalpy, kJ/kg; $\left(\frac{\dot{Q}_{Separator}}{T_0}\right)$ is the heat exchanged between the separator and environment, kW; and $\dot{I}$ is the separator exergy waste, kW.

The equations of tap valve exergy are as follows (Jafari et al., 2012):

$$\dot{E}_{S.T.V.} = \dot{m}_5 (e_6 - e_5) + \left[\left(1 - \frac{T_0}{T_{T.V.}}\right)\dot{Q}_{T.V.}\right] \quad (56)$$

$$\dot{S}_{gen.T.V.} = \dot{m}_5 (s_6 - s_5) - \left(\frac{\dot{Q}_{T.V.}}{T_0}\right) = \dot{m}_5 \left[s_6 - s_5 - \left(\frac{\dot{Q}_{T.V.}}{T_{Source}}\right)\right] \quad (57)$$

$$\dot{S}_{gen.T.V.} = \dot{m}_5 \left[s_6 - s_5 - \left(\frac{h_6 - h_5}{T_{Source}}\right)\right] \quad (58)$$

$$\dot{I} = T_0 \times \dot{S}_{gen.T.V.} = \dot{m}_5 \times T_0 \left[s_6 - s_5 \left(\frac{h_6 - h_5}{T_{Source}}\right)\right] \quad (59)$$

where $\dot{E}_{S.T.V.}$ is the tap valve exergy flow, kW; T_0 and $T_{T.V.}$ are ambient temperature and tap valve temperature, respectively, K; $\dot{Q}_{T.V.}$ is the tap valve heat level, kW; $\dot{S}_{gen.T.V.}$ is the tap valve net rate of entropy change, kW/K; e_5 and e_6 are the tap valve inlet and outlet exergy, kJ/kg; $\dot{m}_5$ is the tap valve inlet mass discharge, kg/s; s_5 and s_6 are the tap valve inlet and outlet entropy, kJ/(kg·K); h_5 and h_6 are the tap valve inlet and outlet enthalpy, kJ/kg; $\left(\frac{\dot{Q}_{T.V.}}{T_0}\right)$ is the heat exchanged between the tap valve and environment, kW; and $\dot{I}$ is the tap valve exergy waste, kW.

The total exergy waste equation is as follows:

$$\sum \dot{I}_{total} = \dot{I}_{Pump} + \dot{I}_{Turb.1} + \dot{I}_{Turb.2} + \dot{I}_{Cond.1} + \dot{I}_{Cond.2} + \dot{I}_{Eva} + \dot{I}_{Sep} \quad (60)$$

where $\dot{I}_{Pump}$ is the pump exergy waste, kW; $\dot{I}_{Turb.1}$ is the turbine 1's exergy waste, kW; $\dot{I}_{Turb.2}$ is the turbine 2's exergy waste, kW; $\dot{I}_{Cond.1}$ is the condenser 1's exergy waste, kW; $\dot{I}_{Cond.2}$ is the condenser 2's exergy waste , kW; $\dot{I}_{Eva}$ is the heat exchanger exergy waste, kW; and $\dot{I}_{Sep}$ is the separator exergy waste, kW.

The exergy efficiency equations are as follows:

$$\dot{E}x_{useful\ output} = \left[\left(\dot{W}_{Turb.1} + \dot{W}_{Turb.2}\right) - \dot{W}_{Pump}\right] \quad (61)$$

$$\dot{E}x_{in} = \sum \dot{I}_{total} + \dot{W}_{net} \quad (62)$$

$$\eta_{ex} = \left[\frac{\left[\left(\dot{W}_{Turb.1} + \dot{W}_{Turb.2} \right) - \dot{W}_{Pump} \right]}{\sum \dot{I}_{total} + \dot{W}_{net}} \right] \quad (63)$$

where η_{ex} is the exergy efficiency, %; $\dot{E}x_{useful\ output}$ is the system useful exergy output, kW; $\dot{W}_{Turb.1}$, $\dot{W}_{Turb.2}$, $\dot{W}_{Pump}$ and $\dot{W}_{net}$ are the turbine 1, turbine 2, pump and total power, respectively, kW; and $\sum \dot{I}_{total}$ is the total exergy waste, kW.

5. The economic study of geothermal power plant

The economic analysis includes the calculation of the components costs and the purchased equipment, maintenance costs, performance, and the consumed energy. The thermos-economic analysis is a study on the economic principles with the purpose of exergy analyses of the studied system. The thermo-economic analysis is applied by the equilibrium equation for the cost of components in the system. This equation is as follows (Lukawski et al., 2016):

$$\sum_{out} \dot{C} + \dot{C}_W = \sum_{in} \dot{C} + \dot{C}_Q + \dot{Z} \quad (64)$$

where $\dot{C}$ is the total costs and indicates the exergy flow value of a specific component of the system (US$); $\dot{C}_W$ and $\dot{C}_Q$ are the total costs and exergy flow value produced by system power and heat (US$); $\dot{Z}$ is the total yearly investment costs of the system (US$); and in and out subscripts stand for input and output.

The total costs and exergy flow value produced by a system's specific component power and heat are as the following equations:

$$\dot{C}_{out} = c_{out} \times \dot{E}x_{out} \quad (65)$$

$$\dot{C}_{in} = c_{in} \times \dot{E}x_{in} \quad (66)$$

$$\dot{C}_W = c_W \times \dot{W} \quad (67)$$

$$\dot{C}_Q = c_Q \times \dot{E}x_Q \quad (68)$$

where c is the average costs of each unit of exergy (US$); $\dot{C}_{in}$ and $\dot{C}_{out}$ are the total costs and expression of the input and output exergy flow of a specific component of the system (US$); $\dot{C}_W$ and $\dot{C}_Q$ are the total costs and exergy flow value produced by a system's specific component power and heat (US$); c_W and c_Q are the average costs of each unit of exergy produced by a system's specific component power and heat (US$); $\dot{E}x_Q$ is the exergy waste by the heat in a specific component of system, kW; $\dot{W}$ is the power of a specific component of system, kW; and in and out subscripts stand for input and output. The value of the exergy amount in this equation is based on the analysis of exergy in the system.

The total costs of the proposed system is expressed as a function of the total costs of fuel and the annual cost of investment, and is as follows (Lukawski et al., 2016):

$$\dot{C}_{P.total} = \dot{C}_{fuel} + \dot{Z}_{total} \quad (69)$$

where $\dot{C}_{P.total}$ is the total costs of the system (US$); $\dot{C}_{fuel}$ is the total fuel costs (US$); and $\dot{Z}_{total}$ is the total annual investment costs of system (US$).

The cost of exergy waste in each component of the system is calculated based on the costs of these components, which is as follows (Lukawski et al., 2016):

$$\dot{C}_D = c_p \times \dot{E}x_d \quad (70)$$

where $\dot{C}_D$ is the cost of exergy waste in a specific component of system (US$); c_p is the average costs of each unit of exergy in a specific component of system (US$); and $\dot{E}x_d$ is exergy waste in a specific component of system, kW.

The thermo-economic coefficient and the dependent cost difference of each component of the system are as the following equations (Lukawski et al., 2016):

$$r = \left[\frac{c_P - c_F}{c_F} \right] \quad (71)$$

$$f = \left[\frac{\dot{Z}}{\left(\dot{Z} \right) + c_F \dot{E}x_d} \right] \quad (72)$$

where r is the dependent cost difference, c_F and c_P are the costs of an exergy unit dependent on production and fuel stream of a specific component of system, respectively (US$); f is the thermos-economic coefficient; $\dot{Z}$ is the annual investment costs of the system (US$); and $\dot{E}x_d$ is the exergy waste of a specific component of system, kW.

The costs of an exergy unit dependent on production and fuel stream of a specific component of system are calculated as follows (Lukawski et al., 2016):

$$c_P = \left[\frac{\dot{C}_P}{\dot{E}x_P} \right] \quad (73)$$

$$c_F = \left[\frac{\dot{C}_F}{\dot{E}x_F} \right] \quad (74)$$

where c_F and c_P are the costs of exergy unit dependent on the fuel and production of a specific component of system (US$); $\dot{C}_P$ and $\dot{C}_F$ are the production and fuel costs for a specific component of system (US$); $\dot{E}x_P$ and $\dot{E}x_F$ are production and fuel exergy in a specific component of system, kW.

The annual investment costs for all the components of system are calculated by the sum annual investment costs of the system and the maintenance costs. Total Capital Investment (TCI) includes two parts as Direct Capital Cost (DCC) and Indirect Capital Cost (ICC). The DCC includes the Purchase Equipment Cost (PEC) and is a function of some designing parameters. The ICC can be taken as a function of PEC or a

function of design parameters and operational conditions. The analysis and calculation of the PEC is taken as a function of components design parameters. By the use of these analyses, the relations between the turbine output power, pump power, and the surface area of the heat exchanger can be explained (Lukawski et al., 2016). The use of geothermal sources, like the other fossil fuels, requires heavy investments for exploration, drilling, expansion of the geothermal field, and purchasing the power plant equipment. The total costs of the initial investment on the plant is a function of plant equipment and facilities purchase costs, the costs of drilling and completion of production and injection wells, the geothermal field exploration and the use of the land for power plant, and the costs of piping for transferring the geothermal fluid from the well to the power plant. The total investment costs of the power plant are as follows (Lukawski et al., 2016):

$$\begin{aligned} &Direct\ Capital\ Cost \\ &= [(1+0.68) \times Purchase\ Equipment\ Cost] \end{aligned} \tag{75}$$

$$Indirect\ Capital\ Cost = [0.14 \times Direct\ Capital\ Cost] \tag{76}$$

$$\begin{aligned} &Total\ Investment \\ &= [(1+0.15) \times (Direct\ Cost + Indirect\ Cost)] \end{aligned} \tag{77}$$

$$\Phi = \left[\left(1+\sum fi\right) f\frac{1}{E}\Phi_E + f\frac{1}{S}\Phi_S + f\frac{1}{W}\Phi_W + f\frac{1}{F}\Phi_F\right] \tag{78}$$

where $Direct\ Cost$ is the power plant direct costs (US$); $Purchase\ Equipment\ Cost$ is the expenditure for purchasing the plant's equipment (US$); $Indirect\ Capital\ Cost$ is the indirect plant's investments (US$); and $Total\ Capital\ Investment$ is the total consequential costs of system investment (US$); Φ is total investment costs of the system (mUS$); fi is the power plant DCC coefficient including the equipment, installation, and building costs; $f\frac{1}{E}$, $f\frac{1}{S}$, $f\frac{1}{W}$ and $f\frac{1}{F}$ are power plant ICC coefficient for equipment, exploration, drilling operations, and transference of geothermal fluid, respectively; Φ_E, Φ_S, Φ_W and Φ_F are the costs of power transmission unit equipment and facilities, exploration costs, drilling operation costs, and geothermal fluid transference costs (mUS$), respectively. The cost of equipment and facilities of power transmission unit includes the purchase of turbines, heat exchangers, pumps, and so on. In this method, the system is broken down into its base equipment, and the calculations of each section are done according to the appropriate economic analysis. Then, other costs, such as installment costs, indirect costs, and potential costs are added to it. The first step in calculating the total investment cost is to calculate the price of each equipment. However, in most cases due to lack of sufficient information about the price of a given device, the costs are calculated by the use of existing relationships and the reference prices (Ram et al., 2013).

The equation of initial costs of purchasing turbine equipment are as follows (Akın et al., 2010):

$$\begin{aligned} \log_{10}(PEC_{Turb}) = K_{1.Turb} + K_{2.Turb}\left(\log_{10}\dot{W}_{Turb}\right) \\ + K_{3.Turb}\left(\log_{10}\dot{W}_{Turb}\right)^2 \end{aligned} \tag{79}$$

where $\dot{W}_{Turb}$ is the turbine power, kW; $K_{1.Turb}$, $K_{2.Turb}$ and $K_{3.Turb}$ are the turbine equipment costs coefficient, US$; and PEC_{Turb} is the initial costs of purchasing the turbine equipment (US$).

The equation of initial costs of purchasing the heat exchanger is as follows (Akın et al., 2010):

$$\begin{aligned} \log_{10}(PEC_{HE}) = K_{1.HE} + K_{2.HE}(\log_{10}A_{HE}) \\ + K_{3.HE}(\log_{10}A_{HE})^2 \end{aligned} \tag{80}$$

where A is the heat exchanger surface area, m^2; $K_{1.HE}$, $K_{2.HE}$ and $K_{3.HE}$ are the heat exchanger equipment costs coefficients (US$); and PEC_{HE} is the initial costs of heat exchanger equipment (US$).

The equation of initial costs of purchasing the pump equipment are as follows (Akın et al., 2010):

$$\begin{aligned} \log_{10}(PEC_{Pump}) = K_{1.Pump} + K_{2.Pump}\left(\log_{10}\dot{W}_{Pump}\right) \\ + K_{3.Pump}\left(\log_{10}\dot{W}_{Pump}\right)^2 \end{aligned} \tag{81}$$

where $\dot{W}_{Pump}$ is the pump power, kW; $K_{1.Pump}$, $K_{2.Pump}$ and $K_{3.Pump}$ are the pump equipment purchase costs coefficients (US$); and PEC_{Pump} is the initial costs of the pump equipment purchase (US$). The constant values for calculation of the Damavand Power Plant equipment costs are presented in Table 4.

Table 4. Constant values for calculation of the Damavand Power Plant equipment costs.

Economic constant	HEX	PUMP	TURBINE
K_1	0.3892	3/3892	2.6559
K_2	0.1557	0/0536	1.4398
K_3	-0.1547	0-/1538	-0.1776

The exploration and access to the geothermal reservoir are very costly, and its capacity is so important, especially if the area in question is not subject to preliminary examination and indications of the presence of geothermal energy such as hot springs and altered areas due to geothermal fluid on the Earth's surface are not visible. Geothermal energy exploration includes geological, hydrogeological, geochemistry, geophysical studies, and the drilling of a thermo-experimental well, which increases the cost of this operation, respectively. Also, the cost of purchasing and the right to use the land for the drilling the wells and land of the plant is also included in this cost. The effects of these costs are so important and significant since

these costs should be paid far before any exploitation (Ram et al., 2013). In the estimation of productive and injection well drilling operational costs, many factors should be considered. The drilling costs are a function of the number of the wells, the depth of the wells, the well's diameter, the type of stone, the distance between the wells, the access ways to the place of drilling, and so on. The costs of experiments, drilling mud, cementing, and piping also included in drilling costs. The number of production wells needed for supplying the power plant steam is variable, depending on the wells efficiency and the amount of steam needed for each megawatt is calculated as around 6 to 7 ton/h (Ram et al., 2013).

The costs of drilling a geothermal well are calculated as follows (Beckers et al., 2013):

$$Drilling\ Costs = 1.65 \times 10^{-5} z^{1.607}\ (1600 < z < 9000m) \tag{82}$$

where $Drilling\ Costs$ is the costs of well-drilling (mUS$); and z is the depth of the well, m. The costs of piping for transmission of the subterraneous fluid between the wells and different parts of the plant and the related pumps system, is a function of the distance between the production wells, the power transmission unit, the diameter of the pipes which is determined based on the fluid discharge and pressure, and the percentage of insulation and the composition of the geothermal fluid (corrosion and precipitation in the pipes) (Mozafari and Ehyaei, 2012). The operational costs include the exploitation and maintenance costs which are considered 4% of the total initial costs and is as the following equation (Ram et al., 2013).

$$OM = \sum_{t=1}^{25} \frac{0.04 \times total\ cost}{(1+0.08)^t} \tag{83}$$

where OM is the operational costs including the exploitation and maintenance costs (US$); $total\ cost$ is the total investment costs of power plant (US$); and t is the year of the power plant.

The electrical power generation costs are as follows (Ram et al., 2013):

$$S = \frac{1}{N}\left\{ i \left(\frac{S_E(i+1)^{n_E}}{(1+i)^{n_E}-1} + \frac{S_s(i+1)^{n_S}}{(1+i)^{n_S}-1} + \frac{S_W(i+1)^{n_W}}{(1+i)^{n_W}-1} + \frac{S_F(i+1)^{n_F}}{(1+i)^{n_F}-1} + OM \right) \right\} \tag{84}$$

$$N = 8760 \times CF \times P_o \tag{85}$$

where S is the electrical power generation costs (US$); N is the annual produced power, kW/h; S_E, S_S, S_W and S_F are the costs of power transmission unit equipment, exploration, drilling operations, and transmission of geothermal fluid, respectively (US$); CF is the power plant capacity coefficient, %; P_o is the plant's power, kW; OM is the operational costs including the exploitation and maintenance costs (US$); i is the discount rate, %; and n_E, n_S, n_W and n_F are the capital return time for the power transmission unit equipment, exploration, drilling operations, and transmission of geothermal fluid, year, which is considered to be equal to the life span of the mentioned parts. Table 5 presents the values of parameters for calculating the cost of electrical power generation in Damavand Power Plant.

Table 5. The values of parameters for calculating the cost of electrical power generation in Damavand Power Plant.

i	[%]	10
P	[MW]	2
CF	[%]	80
n_E	[year]	20
n_S	[year]	50
n_W	[year]	12
n_F	[year]	20

Levelized cost of energy in the power plant are as follows:

$$LCOE = \left[\frac{\sum_{t=1}^{n} \left(\frac{I_t + M_t + F_t}{(1+r)^t} \right)}{\sum_{t=1}^{n} \left(\frac{E_t}{(1+r)^t} \right)} \right] \tag{86}$$

where $LCOE$ is the Levelized Cost of Energy in the power plant in year t (US$); I_t is the total investment costs in year t, (US$); M_t is the operational costs including exploitation and maintenance costs in year t (US$); F_t is the fuel cost in year t (US$); E_t is the electrical power generated in year t, kW/h; r is the discount rate, %; and n is the life span of power plant, year. One of the most important concepts that govern the operation of a power plant is the operating efficiency determined by the difference in temperature between the boiler and the condenser.

The theoretical efficiency of the cycle is as follows:

$$TEC = \left[\frac{T_n - T_1}{T_n} \right] \times 100 \tag{87}$$

where TEC is the theoretical efficiency of the cycle, %; T_n is the absolute temperature of the steam discharged by the boiler, K; T_1 is the absolute temperature of the condenser, K. The absolute temperature is determined by adding 273 to the temperature at ^{o}C.

6. Results and discussion

The MATLAB software was used for solving the dominant thermodynamic equations. After writing all the equations, the error and trial method was used for calculation of the answers in this written code. Indeed, to calculate the thermo-physical properties of the fluid, the MATLAB software was used, by which the thermo-physical properties were calculated for a wide range of temperatures and pressures. After calculation of the thermo-physical properties of the fluid with the MATLAB software, these specifications were placed in the Excel table. Finally, these files were restored by MATLAB software and

Table 6. Thermodynamic properties of different cycle components.

	T[^{o}C]	P[kPa]	s[kJ·kg^{-1}·K^{-1}]	h[kJ·kg^{-1}]
1	56.8	274	2.7	372.5
2	36.2	265	1.56	240.42
3	38.4	310	2.18	243.08
4	109.9	300	2.65	385.47
5	150	4545	1.84	632.18
6	126.1	4410	1.58	524.96
7	114.8	4278	1.47	482.46
8	110	4278	1.41	461.27
9	51.6	324.7	0.71	209.31
10	46.3	315	0.63	191.4
11	110	315	1.52	503.96
12	20	393.1	0.30	83.94
13	43.1	316.2	0.61	179.75
14	20	393.1	0.30	83.94
15	43.1	316.2	0.61	179.75

their information was used. Also, for the water properties, the existing models were used which properly modeled the water properties in saturated and unsaturated modes. In the geothermal system, the temperature of the fluid output from the earth is the main variable affecting the complex function. In this regard, the effect of geothermal fluid temperature on the total thermal efficiency of the plant can be estimated by the following equation:

$$\eta_{th} = [0.0935(T) - 2.3266] \tag{88}$$

where η_{th} is the thermal efficiency of the plant, %; T is the geothermal fluid temperature, ^{o}C. The following equation provides the change in geothermal fluid temperature based on the change in the well's depth (Garcia-Estrada et al., 2001; Quoilin et al., 2011):

$$T = [83.92\ln(z) - 361.16] \tag{89}$$

where z is the well's depth, m; and is the geothermal fluid temperature, ^{o}C. By the use of this equation, the effect of well's depth on the fluid's temperature can be shown in the modeling of the system. In this regard, the effect of well's depth on the output fluid temperature and power plant's efficiency is determined. The well's depth is a sensitive variable with many constraints such as high technology and costs (Garcia-Estrada et al., 2001; Quoilin et al., 2011). To validating the results, the same condition of Yousefi and Ehyaei (2017) as considered as input information of computer program. By comparison the results, average errors of first and second law efficiencies are about 4.5% and 5.7%, respectively. The Table 6 to Table 10 provide the thermodynamic properties of different cycle components, mass discharge of the cycle's working fluid, results of economic analysis of the cycle, results from thermodynamic analysis of cycle, and total cost of investment in Damavand geothermal power plant, respectively. The results of the written code were compared to those of reference number 50 and the maximum error value was

Table 7. Mass discharge of the cycle's working fluid.

Cooling water flow	$\dot{m}_{cw}$	[kg·s^{-1}]	35.6
Geothermal flow	$\dot{m}_{HF}$	[kg·s^{-1}]	15
Organic flow	$\dot{m}_{OF}$	[kg·s^{-1}]	12

Table 8. Results of economic analysis of the cycle.

Condenser 1 area	A_{Cond}	[m^2]	706.9
Condenser 2 area	A_{Cond}	[m^2]	740.6
HX area	A_{Eva}	[m^2]	415.1
Total area	A_{Tot}	[m^2]	1863
Exergy cost component	c_P	[$]	99.64
Production cost of system component	$\dot{C}_P$	[$]	5379

Table 9. Results from thermodynamic analysis of cycle.

HX heat transfer rate	$\dot{Q}_{Eva}$	[MW]	10.83
Condenser 1 heat transfer rate	$\dot{Q}_{Cond.1}$	[MW]	9.31
Condenser 2 heat transfer rate	$\dot{Q}_{Cond.2}$	[MW]	9.8
Turbine 1 power production	$\dot{W}_{Turb.1}$	[MW]	1.03
Turbine 2 power production	$\dot{W}_{Turb.2}$	[MW]	1.14
Pump power production	$\dot{W}_{Pump}$	[MW]	0.156
Total entropy rate	$\dot{S}_{gen}$	[MW·K^{-1}]	172.97
Energy efficiency	η_{th}	[%]	18.25
Exergy efficiency	η_{ex}	[%]	21.3
Turbine 1 energy efficiency	$\eta_{h.Turb.1}$	[%]	84.9
Turbine 2 energy efficiency	$\eta_{h.Turb.2}$	[%]	81.3
Pump energy efficiency	$\eta_{h.Pump}$	[%]	79.7
Specific power	w	[kJ·kg^{-1}]	31.43

Table 10. Total cost of investment in Damavand Geothermal Power Plant.

Cost of preliminary exploration of the power plant	-	[m$]	0.01	1.0
Cost of preliminary feasibility studies for the plant	-	[m$]	0.58	1.9
Cost of preliminary feasibility studies for the plant	-	[m$]	0.12	1.3
Cost of equipment and units of power transmission	Φ_E	[m$]	3.60	37.4
Cost of exploration	Φ_S	[m$]	0.06	0.7
Cost of drilling operations of the power plant	Φ_W	[m$]	1.04	10.8
Cost of transferring underground fluid from Power Plant	Φ_F	[m$]	1.05	10.9
Cost of installing equipment and building a power plant	-	[m$]	0.08	0.9
Cost of construction a well geothermal	-	[m$]	0.05	0.5
Direct cost of power plant	DCC	[m$]	0.05	0.5
Indirect cost of power plant	ICC	[m$]	0.67	6.9
Possible cost of power plant	ECC	[m$]	0.15	1.6
Total cost of power plant	TCI	[m$]	0.09	0.9
Operation cost of power plant	OM	[m$]	0.34	3.5
Cost of operation and construction	-	[m$]	1.53	15.9
Cost of electricity transmission to Damavand Power Station	-	[m$]	0.44	4.6
Cost of hot water transfer to the central heating system	-	[m$]	0.06	0.6
Cost of purchasing postal distribution devices	-	[m$]	0.03	0.3
Total investment cost of Power Plant	-	[m$]	9.64	100

obtained around 5.7% (Li et al., 2016).

The Fig. 3 represents the amount of entropy produced by different components of Damavand Power Plant's geothermal cycle. According to the figure, it can be concluded that the highest entropy production belongs to the heat exchanger and the lowest entropy production belongs to the heat pump. In fact, the highest entropy we produced in heat exchanger due to transmission of heat and the lowest is produced in the fluid pump. The Fig. 4 represents the percentage of exergy waste in different components of the geothermal cycle of Damavand Power Plant. Similar to the previous figure, the highest and lowest exergy waste belong to the heat exchanger and the heat pump, respectively. The Fig. 5 shows the costs of the exergy waste for each of components of the Damavand Power Plant geothermal cycle. Contrary to the previous figures, the highest costs of exergy waste, regarding the high price of the turbine compared to the heat exchanger, belongs to the turbine and the lowest costs again belong to the heat pump.

Fig. 6 represents the exergy-economic coefficient for different components of the geothermal cycle of Damavand Power Plant. The highest coefficient belongs to the pump and the lowest coefficient belongs to the condenser 1. However, it can be concluded from the range of variations for the various components of the cycle is roughly constant.

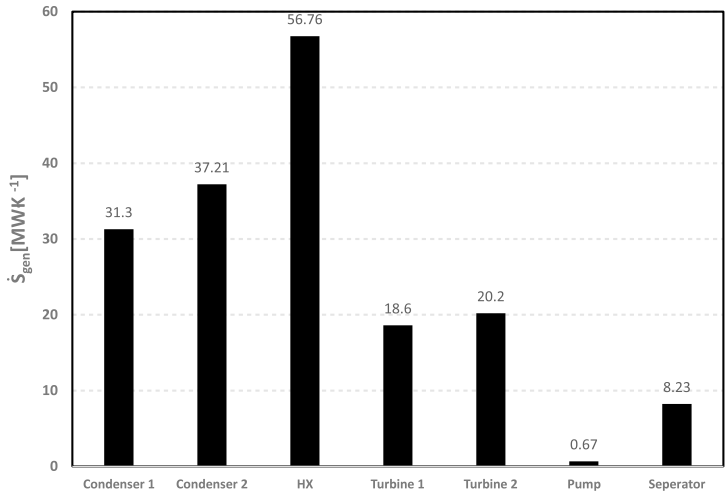

Fig. 3. Amount of entropy produced by different components of Damavand Power Plant's geothermal cycle.

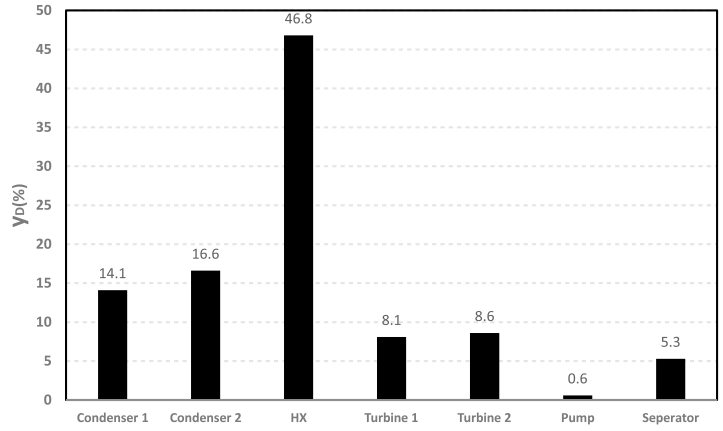

Fig. 4. Percentage of exergy waste in different components of geothermal cycle of Damavand Power Plant.

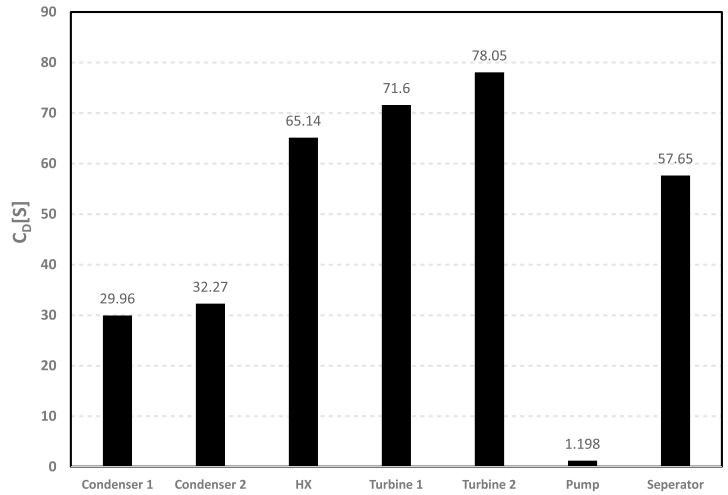

Fig. 5. Costs of the exergy waste for each of components of the Damavand Power Plant geothermal cycle.

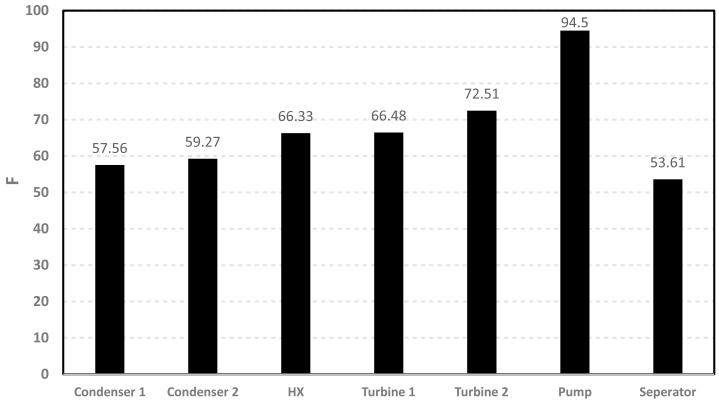

Fig. 6. Exergy-economic coefficient for different components of geothermal cycle of Damavand Power Plant.

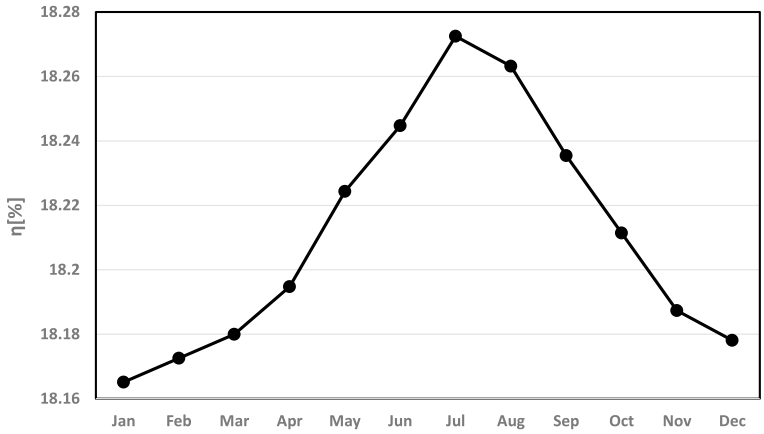

Fig. 7. Changes in geothermal cycle's energy efficiency in different months of the year.

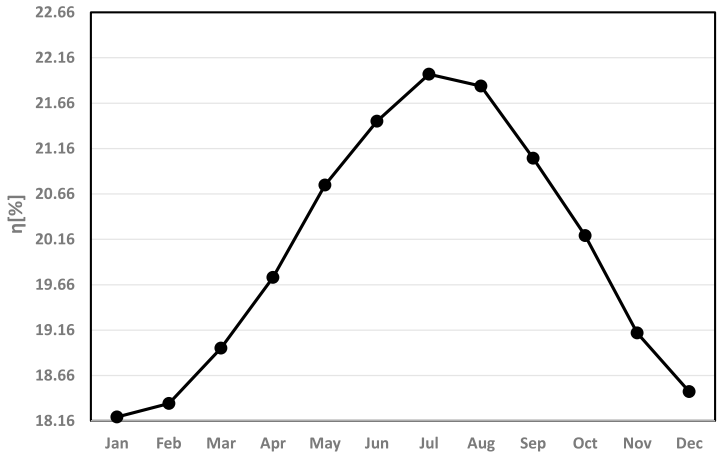

Fig. 8. Changes in geothermal cycle's exergy efficiency in different months of the year.

The Fig. 7 and Fig. 8 show the changes in energy and exergy efficiencies in different months of the year, respectively. It is obvious that the changes in temperature does not significantly affect the system performance. However, the effects of these temperature changes is more manifested in exergy efficiency, but it can be ignored in both modes.

7. Conclusion

The current study aimed at optimization of an ORC with geothermal source based on the thermodynamic and economic analysis of Damavand district for simultaneous production of heat energy needed for the central heating system and electrical power for the network of Damavand City and a part of Tehran province as well as reduction of the economic costs and increasing the efficiency of the mentioned power plant. The results of the current study are as follows:

1) The organic working fluid for the above mentioned cycle is R245fa which is a non-flammable and a slightly dry fluid. This fluid has a low latent heat as well as a low specific volume. It has also proper environmental properties such as zero Ozone depletion capacity and a low thermal capacity and it is an appropriate superheater on the output of the heat exchanger.

2) The estimation of the costs of drilling a well and designing and erecting a 2 MW geothermal power plant in Damavand district were 1.04 and 9.64 (mUS$), respectively. These estimates, compared to the Nesjavellir geothermal power plant in Island, show a reduction in costs as 6.1% and 7.4%, respectively.

3) The return of capital period for Damavand Geothermal Power Plant was calculated as 15 years.

4) The power generation cost for Damavand Geothermal Power Plant is 17 cents per each kWh.

5) The values of energy efficiency, exergy efficiency, the net rate of entropy change, and the specific output power were calculated as 18.2%, 21.3%, 172.97 kW/K, and 31.43 kJ/kg, respectively, for the ORC with geothermal heat source.

6) The highest and lowest entropy for the ORC with geothermal heat source were 56.8 MW/K and 16.8 MW/K, which belonged to the heat exchanger and the pump, respectively.

7) The highest and lowest amounts of the costs of exergy waste in the ORC with geothermal heat source were 78.1 and 1.2 (US$), for the turbine and pump.

8) The results indicated that since the change in the temperature is tiny, it has little effects on the temperature change at different stages as well as the energy efficiency and the output temperature of the cycle. The only significant effect the temperature changes have is on the exergy efficiency of ORC with the geothermal heat source, which is around 2% of the changes based on the climate changes, during a year.

Nomenclature

A = area, m^2
B_1, B_2 = bare module factor of equipment
C = cost rate, \$
$CLEF$ = Constant Escalation Levelization Factor
C_1, C_2, C_3 = perssure factor of equipment
CF = Capacity Factor, %
c = cost per exergy unit, \$
DS = Dry Steam
DFC = Double Flash Condensing
DCC = Direct Capital Cost, \$
DC = Drilling Cost, \$
d = diagonal, mm
$\dot{E}$ = exergy rate, kW
$\dot{E}_D$ = exergy destruction, kW
e = specific exergy, $kJ \cdot kg^{-1}$
F = Factor
f = exergoeconomic factor, %
GWP = Global Warming Potential
gZ = potential energy, m
H = height, m
h = enthalpy, $kJ \cdot kg^{-1}$
ICC = Indirect Capital Cost, \$
i = interest rate, %
K_1, K_2, K_3 = coefficients of equipment cost, \$
L = length, m
$\dot{m}$ = mass flow rate, $kg \cdot s^{-1}$
N = annual electricity genrative, $kW \cdot h^{-1}$
$OTEC$ = Ocean Temperature Energy Conversion
ORC = Organic Rankine Cycle
$ORCR$ = Organic Rankine Cycle Regenerator
$ORCP$ = rganic Rankine Cycle Paralell
$ORCS$ = Organic Rankine Cycle Serial
OM = Operating Cost, \$
ODP = Ozone Depletion Potential
P_o = Power, MW
P = perssure, Bar, MPa
PEC = Purchase Equipment Cost, \$
$\dot{Q}$ = Heat rate, kW
r = relative cost difference
S = electricity cost, \$
SFB = Single Flash Backpressure
SFC = Single Flash Condensing
$\dot{S}_{gen}$ = entropy generation, $kW \cdot K^{-1}$
s = specific entropy, $kJ \cdot kg^{-1} \cdot K^{-1}$
T = temperature, ^oC, ^oK
TCI = Total Capital Investment, \$
V = volume, m^3
V = kinetic energy, $m \cdot s^{-1}$
$\dot{W}$ = work, kW
w = specific power, $kJ \cdot kg^{-1}$
y = exergy destruction rate, %
$\dot{Z}$ = annual investment cost rate, \$
ε = heat transfer effectiveness, -
η = efficiency, %

Subscripts

con = Condenser
cw = cooling water
D = destruction
E = Equipment

El = Electricity
ex = exergy
eff = effective
eva = Evaporator
F = Fuel
geo = Geothermal
gen = generation
gf = geothrmal fluid
HE = Heat Exchanger
HF = Heat Fluid
in = inlet
is = isentropic
M = material
max = maximal
min = minimal
net = net
OF = Organic Fluid
out = outlet
P = pressure
pin = pinch point
pum = Pump
Q = heat
rec = Recuperator
S = discovery
sep = Separator
sin = sink
sou = source
$stag$ = stagnation
th = thermal
tot = total
tur = Turbine
use = useful
W = work

References

Ahmadi, A., Ehyaei, M.A. Exergy analysis of a wind turbine. Int. J. Exergy 2009, 6(4): 457-476.

Akın, S., Kok, M.V., Uraz, I. Optimization of well placement geothermal reservoirs using artificial intelligence. Comput. Geosci. 2010, 36(6): 776-785.

Aliehyaei, M., Atabi, F., Khorshidvand, M., et al. Exergy, economic and environmental analysis for simple and combined heat and power IC engines. Sustainability. 2015, 7: 4411-4424.

Arslan, O., Yetik, O. ANN based optimization of supercritical ORC-Binary geothermal power plant: Simav case study. Appl. Therm. Eng. 2011, 31(17): 3922-3928.

Asgari, E., Ehyaei, M.A. Exergy analysis and optimisation of a wind turbine using genetic and searching algorithms. Int. J. Exergy 2015, 16(3): 293-314.

Ashari, G.R., Ehyaei, M.A., Mozafari, A., et al. Exergy, economic, and environmental analysis of a PEM fuel cell power system to meet electrical and thermal energy needs of residential buildings. J. Fuel Cell Sci. Technol. 2012, 9(5): 051001.

Astolfi, M., Romano, M.C., Bombarda, P., et al. Binary ORC (Organic Rankine Cycles) power plants for the exploitation of medium-low temperature geothermal sources-Part B: Techno-economic optimization. Energy 2014, 66(4): 435-446.

Bahrami, M., Hamidi, A.A., Porkhial, S. Investigation of the effect of organic working fluids on thermodynamic performance of combined cycle Stirling-ORC. Int. J. Energ. Environ. Eng. 2013, 4(1): 4-12.

Beckers, K.F., Lukawski, M.Z., Reber, T.J., et al. Introducing geophires v1.0: software package for estimating levelized cost of electricity and/or heat from enhanced geothermal systems. Paper SGP198 Presented at Thirty-Eighth Workshop on Geothermal Reservoir Engineering, Stanford University, Stanford, California, February 11-13, 2013.

Bejan, A., Tsatsaronis, G., Moran, M. Thermal design and optimization. Wiley & Sons, New York, 2006.

Dabirsiaghi, M. Raesons for Damavand mountain characteristics change. Soroush publication, Persian, 2013.

Darvish, K., Ehyaei, M., Atabi, F., et al. Selection of optimum working fluid for Organic Rankine Cycles by exergy and exergy-economic analyses. Sustainability. 2015, 7: 15362-15383.

Drozdz, M. An optimisation model of geothermal-energy conversion. Appl. Energ. 2003, 74(1): 75-84.

Ehyaei, M.A. Estimation of condensate mass flow rate during purging time in heat recovery steam generator of combined cycle power plant. Therm. Sci. 2014, 18(4): 1389-1397.

Ehyaei, M.A., Anjiridezfuli, A., Rosen, M.A. Exergetic analysis of an aircraft turbojet engine with an afterburner. Therm. Sci. 2013, 17(4): 1181-1194.

Ehyaei, M.A., Bahadori, M.N. Internalizing the social cost of noise pollution in the cost analysis of electricity generated by wind turbines. J. Wind Eng. Ind. 2006, 30(6): 521-529.

Ehyaei, M.A., Bahadori, M.N. Selection of micro turbines to meet electrical and thermal energy needs of residential buildings in Iran. Energ. Buildings 2007, 39(12): 1227-1234.

Ehyaei, M.A., Farshin, B. Optimization of photovoltaic thermal (PV/T) hybrid collectors by genetic algorithm in Iran's residential areas. Adv. Energ. Res. 2017, 5(1): 31-55.

Ehyaei, M.A., Hakimzadeh, S., Enadi, N., et al. Exergy, economic and environment (3E) analysis of absorption chiller inlet air cooler used in gas turbine power plants. Int. J. Energ. Res. 2012, 36(4): 486-498.

Ehyaei, M.A., Mozafari, A. Energy, economic and environmental (3E) analysis of a micro gas turbine employed for on-site combined heat and power production. Energ. Buildings 2010, 42(2): 259-264.

Ehyaei, M.A., Mozafari, A., Ahmadi, A., et al. Potential use of cold thermal energy storage systems for better efficiency and cost effectiveness. Energ. Buildings 2010, 42(12): 2296-2303.

Ehyaei, M.A., Mozafari, A., Alibiglou, M.H. Exergy, economic & environmental (3E) analysis of inlet fogging for gas turbine power plant. Energy 2011, 36(12): 6851-6861.

El-Emam, R.S., Dincer, I. Exergy and exergoeconomic analyses and optimization of geothermal Organic Rankine Cycle. Appl. Therm. Eng. 2013, 59(1-2): 435-444.

Enhua, W., Hongguang, Z., Boyuan, F., et al. Optimized performances comparison of organic Rankine cycles for low grade waste heat recovery. J. Mech. Sci. Technol. 2012, 26 (8): 2301-2312.

Garcia-Estrada, G., Lopez-Hernandez, A., Prol-Ledesma, R.M. Temperature-depth relationships based on log data from the Los Azufres geothermal field, Mexico. Geothermics 2001, 30(1): 111-132.

Ghasemian, E., Ehyaei, M.A. Evaluation and optimization of Organic Rankine Cycle (ORC) with algorithms NSGA-II, MOPSO, and MOEA for eight coolant fluids. Int. J. Energ. Environ. Eng. 2018, 9(1): 1-19.

Ghasemi, H., Paci, M., Tizzanini, A., et al. Modeling and optimization of a binary geothermal power plant. Energy 2013, 50(1): 412-428.

Golroodbari, S.A., Kalte, M. Energy and exergy analysis of Organic Rankine Cycle with geothermal resource. Second proceeding of heat and mass transfer, Semnan, 2013.

Heberle, F., Brüggemann, D. Exergy based fluid selection for a geothermal Organic Rankine Cycle for combined heat and power generation. Appl. Therm. Eng. 2010, 30(11-12): 1326-1332.

Imran, M., Usman, M., Park, B.S., et al. Multi-objective optimization of evaporator of Organic Rankine Cycle (ORC) for low temperature geothermal heat source. Appl. Therm. Eng. 2015, 80: 1-9.

Jafari, H., Behbahaninia, S.A., Engarnevis, A. Two-objective optimization using combined cycle power plants waste for heating application. J. Modares Mech. Eng. 2012, 12: 120-132.

Jalilinasrabady, S., Itoi, R., Valdimarsson, P., et al. Flash cycle optimization of Sabalan geothermal power plant employing exergy concept. Geothermics 2012, 43(4): 75-82.

Kanoglu, M. Exergy analysis of a dual-level binary geothermal power plant. Geothermics 2002, 31(6): 709-724.

Kanoglu, M., Bolatturk, A., Yilmaz, C. Thermodynamic analysis of models used in hydrogen production by geothermal energy. Int. J. Hydrogen Energ. 2010, 35(16): 8783-8791.

Kazemi, N., Samadi, F. Thermodynamic, economic and thermo-economic optimization of a new proposed Organic Rankine Cycle for energy production from geothermal resources. Energ. Convers. Manage. 2016, 121: 391-401.

Lavizeh, F. General report on geothermal and related fields in Iran. Tehran: Geological Survey of Iran, 2002.

Li, L., Ge, Y.T., Luo, X., et al. Thermodynamic analysis and comparison between CO_2, transcritical power cycles and R245fa Organic Rankine Cycles for low grade heat to power energy conversion. Appl. Therm. Eng. 2016, 106: 1290-1299.

Lukawski, M.Z., Silverman, R.L., Tester, J.W. Uncertainty analysis of geothermal well drilling and completion costs. Geothermics 2016, 64: 382-391.

Mohammadnezami, M.H., Ehyaei, M.A., Rosen, M.A., et al. Meeting the electrical energy needs of a residential building with a Wind-Photovoltaic hybrid system. Sustainability. 2015, 7: 2554-2569.

Mozafari, A., Ahmadi, A., Ehyaei, M.A. Optimisation of micro gas turbine by exergy, economic and environmental (3E) analysis. Int. J. Exergy 2010, 7(1): 1-19.

Mozafari, A., Ehyaei, M.A. Effects of regeneration heat exchanger on entropy, electricity cost, and environmental pollution produced by micro gas turbine system. Int. J. Green Energy 2012, 9(1): 51-70.

Najafi, G., Ghobadian, B. Geothermal resources in Iran: The sustainable future. J. Renew. Sustain. Energ. Rev. 2011, 15(8): 3946-3951.

Nami, H., Nemati, A., Fard, F.J. Conventional and advanced exergy analyses of a geothermal driven dual fluid Organic Rankine Cycle (ORC). Appl. Therm. Eng. 2017, 122: 59-70.

Quoilin, S., Declaye, S., Tchanche, B.F., et al. Thermo-economic optimization of waste heat recovery Organic Rankine Cycles. Appl. Therm. Eng. 2011, 31(14-15): 2885-2893.

Ozgener, L., Hepbasli, A., Dincer, I. Energy and exergy analysis of the Gonen geothermal district heating system, Turkey. Geothermics 2005, 34(5): 632-645.

Ram, G.N., Shree, J.D., Kiruthiga, A. Cost optimization of stand alone hybrid power generation system using PSO. Int. J. Adv. Res. Electr. Electron. Instrum. Eng. 2013, 2(8): 4048-4057.

Saffari, H., Sadeghi, S., Khoshzat, M., et al. Thermodynamic analysis and optimization of a geothermal Kalina cycle system using Artificial Bee Colony algorithm. Renew. Energ. 2016, 89: 154-167.

Saidi, M.H., Abbassi, A., Ehyaei, M.A. Exergetic optimization of a PEM fuel cell for domestic hot water heater. J. Fuel Cell Sci. Tech. 2005a, 2(4): 284-289.

Saidi, M.H., Ehyaei, M.A., Abbasi, A. Optimization of a combined heat and power PEFC by exergy analysis. J. Power Sources 2005b, 143(1-2): 179-184.

Vélez, F., Segovia, J.J., Martn, M.C., et al. A technical, economical and market review of Organic Rankine Cycles for the conversion of low-grade heat for power generation. Renew. Sust. Energ. Rev. 2012, 16(6): 4175-4189.

Wei, D., Lu, X., Lu, Z., et al. Performance analysis and optimization of Organic Rankine Cycle (ORC) for waste heat recovery. Energ. Convers. Manage. 2007, 48(4): 1113-1119.

Yazdi, B.A., Yazdi, B.A., Ehyaei, M.A., et al. Optimization of micro combined heat and power gas turbine by genetic algorithm. Therm. Sci. 2015a, 19(1): 207-218.

Yazdi, M.R.M., Aliehyaei, M., Rosen, M.A. Exergy, economic and environmental analyses of gas turbine inlet air cooling with a heat pump using a Novel system configuration. Sustainability. 2015b, 7: 14259-14286.

Yousefi, M., Ehyaei, M.A. Feasibility study of using organic Rankine and reciprocating engine systems for supplying demand loads of a residential building. Adv. Build. Energ. Res. 2017, 1-17.

Zarrouk, S.J., Moon, H. Efficiency of geothermal power plants: A worldwide review. Geothermics 2014, 51(3): 142-153.

Zhai, H., Shi, L., An, Q. Influence of working fluid properties on system performance and screen evaluation indicators for geothermal ORC (Organic Rankine Cycle) system. Energy 2014, 74(5): 2-11.